

LINE-TO-RING COUPLING CIRCUIT MODEL AND ITS PARAMETRIC EFFECTS FOR OPTIMIZED DESIGN OF MICROSTRIP RING CIRCUITS AND ANTENNAS

Lei ZHU and Ke WU[#]

POLY-GRAMES Research Center

Departement de Génie Electrique et de Génie Informatique
École Polytechnique de Montréal, C.P. 6079, Succ. Centre Ville
Montréal, Québec, Canada H3C 3A7

ABSTRACT

New de-embedding technique developed with a field-theoretical framework is applied to precisely characterizing line-to-ring coupling structure in the form of a circuit model. This circuit model is able to account for various dynamic parametric effects including frequency-related dispersion, radiation and leakage losses. Results are given for dispersive electrical characteristics of loose and enhanced line-to-ring coupling schemes in terms of susceptance-related J-inverter network. The accurate prediction confirmed by a set of experiments provides a guideline for optimally designing ring-resonators with the distributed transmission line model.

INTRODUCTION

Microstrip ring resonator has received considerable attention in the microwave research community. Its geometrical simplicity and attractive advantages are promising in the design of filters, duplexers, oscillators, mixers and antennas [1-3] although the ring technique was initially proposed for microwave measurements. It is well recognized in these ring-based microwave integrated circuits and antennas that line-to-ring coupling structure is a fundamental circuit element. Adequate and accurate design rules and tools are strongly desired to achieve optimized design of these integrated circuits and antennas, predicting in general frequency response and electrical characteristics of ring-based circuits and devices. Extensive experimental works were carried out to investigate electrical performance and parametric effects of the line-to-ring coupling structure [1-2], however, there has been almost no reported research to date on its accurate circuit model and electromagnetic modeling.

Fig. 1(a) presents the geometry of a conventional ring circuit attached with two loose coupling end-to-side gaps, which are known to suffer from a high

insertion loss. Fig. 1(b) depicts an improved version of the ring circuit in which the line-to-ring coupling strength is enhanced by extending the open-end of each feed line along the ring periphery. However, fields perturbation of the feed lines on the ring resonance in this case is obviously more pronounced with increase of the coupling strength. Electrical performance of these line-to-ring coupling schemes should be characterized for precision circuit design. Generally speaking, a generalized equivalent circuit model can be set up as shown in Fig. 1(c) for describing the electrical characteristics of an arbitrarily shaped coupling structure using the concept of a distributed transmission line model [2] with the coupling network representation.

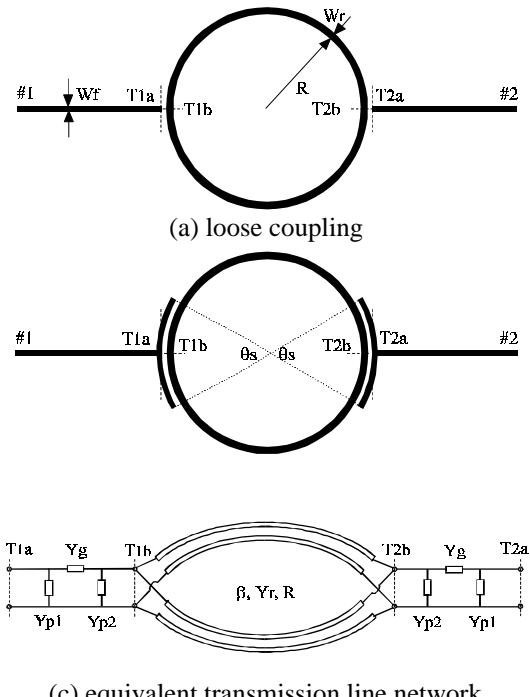


Fig.1 Geometry of the microstrip ring resonator and its equivalent transmission line network

[#] on leave from the above institution and currently with *Telecommunications Research Center, Department of Electronic Engineering, City University of Hong Kong, Tat Chee Avenue, Kowloon, Hong Kong*

To our knowledge, such an equivalent network is usually obtained through some empirical and/or approximate models. It is still very difficult to characterize this three-dimensional (3D) coupling topologies of Fig. 1(a) and (b) in terms of their circuit model parameters extracted by applying electromagnetic modeling/analysis techniques [1]. This unfortunate fact prompts us to develop a new generalized CAD algorithm dedicated to a comprehensive treatment of unbounded line-to-ring coupling structure for its network characterization as shown in Fig. 1(c) designated within the reference planes T_a and T_b .

ENHANCED COUPLING STRUCTURE

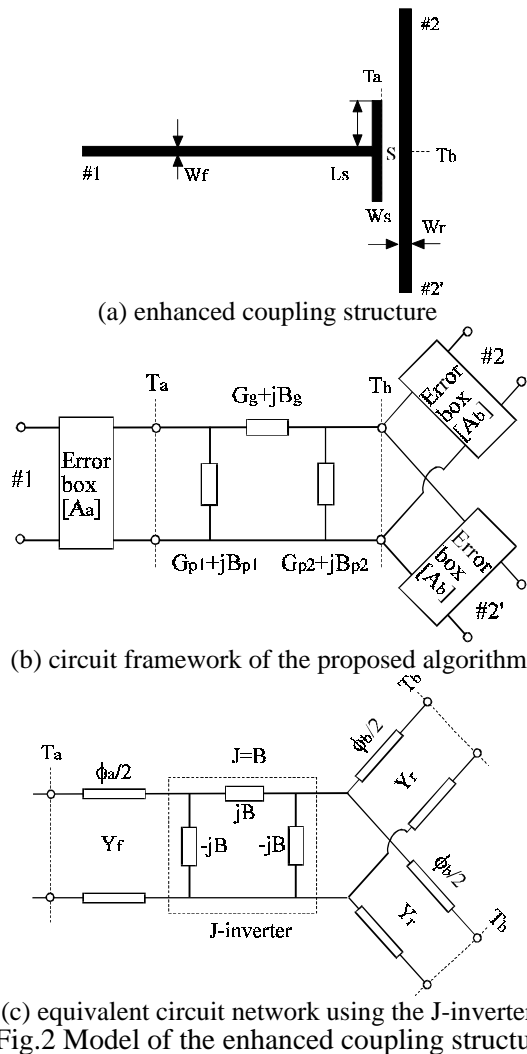


Fig. 2 Model of the enhanced coupling structure

Fig. 2(a) shows a prototype representing the enhanced coupling structure to be theoretically considered for the design of a ring circuit such as Fig. 1(b) whose coupling strength can be essentially controlled by adjusting the stub length L_s of the

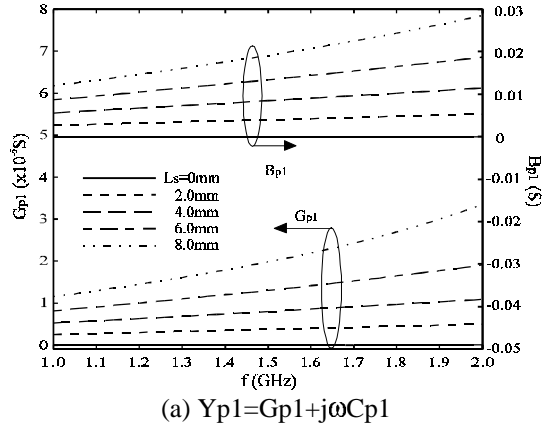
open-end. Fig. 2(b) sketches a unified circuit framework under which a number of built-in circuit parameters involving various dynamic effects are extracted through a new de-embedding technique. This technique that allows to calibrate the core of the coupling circuit and identify potential error terms from the equivalent circuit network. These error terms in this case are directly related to dispersion- and structure-dependent terms mainly brought by the approximation of impressed fields at each line terminal and results consistency between 2D and 3D simulations for numerical modeling of input and output lines. These problems are subject to a particular detail as documented in [4] considering the use of a full-wave moment method.

This de-embedding technique called “Short-Open Calibration (SOC)” technique is used to accurately evaluate the unwanted parasitics reflected in these error boxes as shown in Fig. 2(b). In this way, the realistic circuit model can be established. Fig. 2(c) illustrates an alternative equivalent network topology using the J-inverter susceptance, which can be used to explicitly estimate the line-to-ring coupling characteristics for the purpose of designing an optimized ring circuits with pre-designated circuit performance requirement.

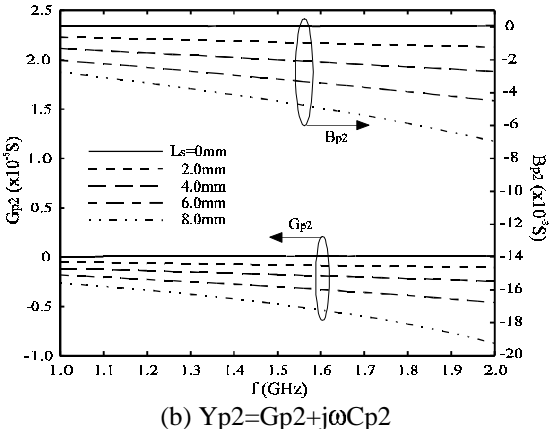
Fig. 3 plots a series of simulated frequency-dependent admittances against various stub length L_s of the input and output lines as defined at the reference planes of concern T_a and T_b . In light of the fact that the coupling structure is unbounded and radiation- and surface-wave related losses may appear, the circuit network is therefore modeled as a lossy network which is generally characterized by two separate sets of self- and mutual-susceptances, namely, B_{p1} , B_{p2} , B_g and self- and mutual conductances G_{p1} , G_{p2} and G_g as indicated in Fig. 2(b).

First, it can be observed from Fig. 3(a), (b) and (c) that results related to the stubless line-to-ring coupling case ($L_s = 0$ mm) remain stationary with respect to frequency. As the stub length L_s increases, G_{p1} and B_{p1} tend to move upward and behave to be linearly dependent with frequency as opposed to G_{p2} and B_{p2} which are shifted into negative values even though their frequency dependency remains similar. The mutual susceptance and conductance show a similar feature compared G_{p1} and B_{p1} . Obviously, the coupling strength is immediately enhanced with a non-zero stub length which allows a distributed coupling taking place symmetrically along the periphery of the line #2 (ring) vis-à-vis the line #1 (feed line). The resulting negative values of G_{p2} and B_{p2} can be well explained by the fact that a stronger mutual coupling leads to a more fringing electric

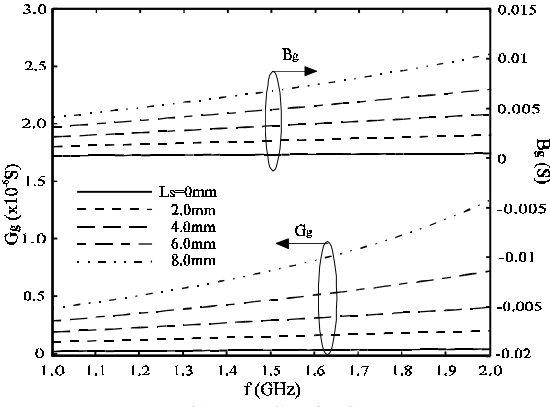
field appearing along the air-dielectric interface between the two lines, thus reducing the effective dielectric constant of the line #2 related to the coupling section. In other words, the guided-wavelength of the line #2 will be increased with the stub length. This can also be perceived by an equivalent inductance effect as far as the coupling characteristics viewed from the reference plane T_b are concerned.



(a) $Y_{p1}=G_{p1}+j\omega C_{p1}$



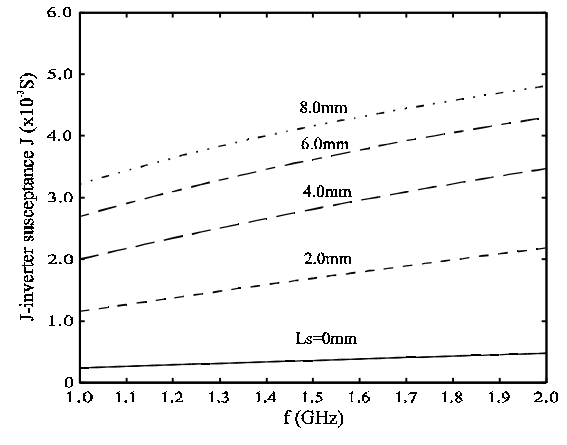
(b) $Y_{p2}=G_{p2}+j\omega C_{p2}$



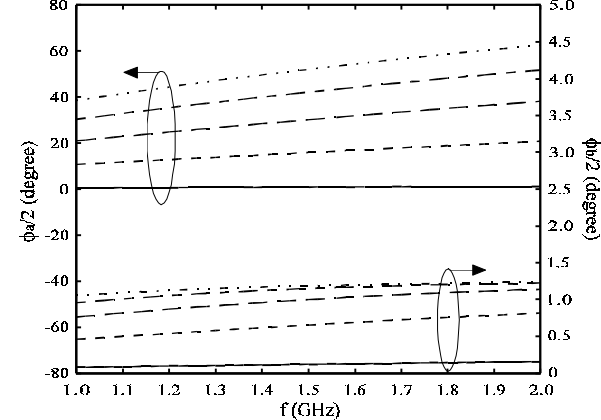
(b) $Y_g=G_g+j\omega C_g$

Fig.3 Simulated dynamic circuit parameters of the enhanced coupling structure

Interestingly, the stub effect is more pronounced at higher frequencies which can be attributed to a more enhanced distributed effect with shorter wavelength for a fixed coupling section. This suggests that the design of a stub-loaded coupling structure be more cautious at relatively higher frequencies. In any case, the total unbounded losses are found to be negligible in the frequency range of interest (1.0 to 2.0 GHz) judging from the conductance values. Therefore, the line-to-ring coupling characteristics can effectively be determined by the simplified J-inverter susceptibility network as illustrated by Fig. 2(c).



(a) J-inverter susceptance

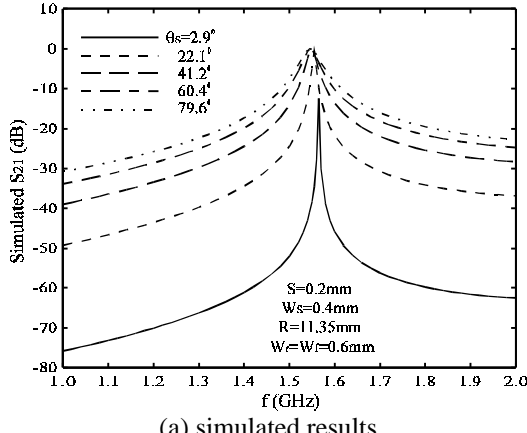


(b) electric length of imaging lines

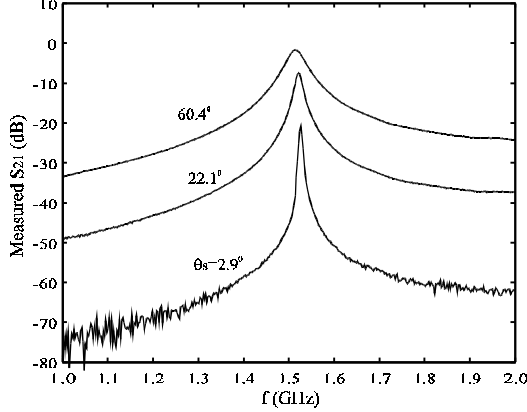
Fig.4 Simulated J-inverter parameters

Fig. 4(a) and (b) show the simulated curves of related J-inverter susceptances and electric lengths of the equivalent network lines which can be easily converted on the basis of the equivalence principal in relation to B_{p1} , B_g , and B_{p2} . It is evident that the J-inverter susceptance can be found in Fig. 4(a) to increase rapidly with the stub length L_s so that the coupling strength is naturally enhanced in a relatively large scale. In line with this observation, the calculated electric length $\phi_b/2$ in connection with

the ring circuit is slightly shifted upward, which can be equivalently conceived as an additional line attached to the line #2 in the circuit model of the ring circuit. Similarly, the other equivalent electric length $\phi_a/2$ is also increased significantly, which characterizes the left-hand side of the J-inverter in connection with the feed line. These characteristics cannot be observed without the use of such an electromagnetic tool in conjunction with the proposed SOC de-embedding technique.



(a) simulated results



(b) measured results

Fig.5 Simulated and measured results of insertion loss for a microstrip ring resonator with different coupling stubs

MICROSTRIP RING RESONATOR

As such, a generalized two-port enhanced line-to-ring coupling topology of Fig. 1(b) can be effectively modeled with the simplified transmission line network as shown in Fig. 1(c) developed in [1-2]. The implied network parameters can be extracted through the proposed rigorous electromagnetic technique.

Fig. 5(a) shows a group of simulated insertion losses for a microstrip ring resonator attached with the

input and output lines loaded with coupling-enhanced stubs L_s which are selected for five cases using the opening angle θ_s notions (see Fig. 1(b)). As the stub length L_s increases (larger θ_s), the insertion loss S_{21} rapidly moves up towards the maximum value (0 dB) around certain frequency. Note that the complete signal transmission for the line-ring-line structure takes place only for strong coupling cases at a particular frequency. The curves of S_{21} become more and more broad and at the same time the resonance frequency of the ring resonator seems to be slightly reduced as the coupling becomes stronger. The towards-saturated enlargement of the curves indicates that the Q-value of the ring resonator is reduced. These phenomena can be very well explained by the above-discussed behavior of the J-inverter susceptance and the equivalent extended line concept. The electric length $\phi_a/2$ contributes significantly to electrical performance of the ring circuit while its counterpart $\phi_a/2$ is merely related to the equivalent extension of the feed lines. To confirm the usefulness and accuracy of the proposed model, experiments are made for three cases corresponding $\theta_s = 2.9^\circ, 22.1^\circ, 60.4^\circ$. The theoretical prediction and measurement results are plotted in Fig. 5(b), showing an excellent agreement between them. In conclusion, the field-theory-based circuit model proposed in this paper is undoubtedly very useful in the accurate design and optimization of ring-based microwave integrated circuits and antennas on the basis of the matured design approaches such as [1, 5]. This powerful technique can also be applied to other forms of circuits and discontinuities including non-planar structures.

REFERENCES

- [1] K. Chang, *Microwave Ring Circuits and Antennas*, Wiley, New York, 1996.
- [2] K. Chang et al., "On the study of microstrip ring and varactor-tuned ring circuits," IEEE Trans. Microwave Theory Tech., vol. MTT-35, no. 12, pp. 1288-1295, Dec. 1987.
- [3] M. Gulielmi and G. Gatti, "Experimental Investigation of dual-mode microstrip ring resonators," Proc. 20th Eur. Microwave Conf., pp. 901-906, Sept. 1990.
- [4] L. Zhu and K. Wu, "Unified dynamic circuit model of planar discontinuities suitable for field theory-based CAD and optimization of M(H)MICs," Submitted to IEEE Trans. Microwave Theory Tech.
- [5] G. Matthaei et al., *Microwave Filters, Impedance-Matching Networks, and Coupling Structures*, Atech House, Norwood, 1980.